Computed micro-tomographic evaluation of glide path with nickel-titanium rotary PathFile in maxillary first molars curved canals.

UNIVERSITÀ DEGLI STUDI DI TORINO

Micro-CT evaluation of glide path with NiTi rotary Pathfile™ in maxillary first molars curved canals.

D. Pasqualini[1], C. Bianchi[2], D. Paolino[3], L. Mancini[4], A. Cemenasco[2], G. Cantatore[5], A. Castellucci[6], E. Berutti[1]

1 Department of Endodontics, University of Turin Dental School, Turin, Italy; 2 Department of Radiodiagnostics University of Turin, 3 Department of Mechanics, Polytechnical School of Turin; 4 Sincrotrone Trieste S.C.p.A, Trieste, Italy; 5 Department of Endodontics, School of Dentistry, University of Verona, Verona, Italy; 6 Department of Endodontics, School of Dentistry, University of Florence, Italy

Conflict of interest: G. Cantatore, A. Castellucci and E. Berutti declare financial involvement (patent licensing arrangements) with Dentsply Maillefer with direct financial interest in the materials discussed in this manuscript.

Address for Correspondence:
Dr. Damiano Pasqualini, via Barrili, 9 – 10134 Torino Italy
Tel: +39(0)11/3184938; Fax: +39(0)11/3184960;
e-mail: damianox@mac.com

Running head: Canal anatomy preservation with glide path

Abstract word count: 250

Text word count: 2224

Tables/Figures: 0/3

Acknowledgements: the authors would like to thank Dr. D. Dreossi and Francesco Brun (Sincrotrone Trieste S.C.p.A) for their valuable support in Micro-CT analysis and Dr. Alovisi and Dr. Calissano (lecturers at the Department of Endodontics, University of Turin Dental School) for their active cooperation.

Abstract

Introduction: Micro-computed-tomography (CT) allows high-resolution 3D imaging of small objects. In this study, micro-CT was used to compare the ability of manual and mechanical glide path to maintain the original root canal anatomy. **Methods:** Eight extracted upper first permanent molars were scanned at the TOMOLAB station with a micro-focus cone beam geometry system. A total of 2400 projections on 360° have been acquired at 100 kV and 80 μA, with focal spot size of 8 micron. Buccal root canals of each specimen (N=16) were randomly assigned to PathFile^{TM} (P) or stainless-steel K-file (K) to perform glide-path at full working length. Specimens were then micro-scanned at apical level (A) and at the point of maximum curvature level (C) for post-treatment analyses. Curvatures of root canals were classified as moderate (≤35°) or severe (≥40°). The ratio of diameter ratios (RDR) and the ratio of cross-sectional areas (RA) were assessed. For each level of analysis (A and C), two balanced two-way factorial ANOVA's ($p<0.05$) were performed to evaluate the significance of the instrument factor and of canal curvature factor, as well as the interactions of the factors both with RDR and RA. **Results:** Specimens in the K group had a mean curvature of 35.4°±11.5°, those in the P group of 38°±9.9°. Instrument factor (P and K) was extremely significant ($p<0.001$) for both the RDR and RA parameters, regardless of the point of analysis. **Conclusion:** Micro-CT confirmed that Ni-Ti rotary Pathfile instruments preserve the original canal anatomy and cause less canal aberrations.

Key words

Micro-CT, Nickel-Titanium, Ni-Ti rotary instrumentation, PathFile, glide path

Nickel-titanium (Ni-Ti) rotary instruments reduce operator fatigue, time required for shaping and risk of procedural errors associated with root canal instrumentation (1,2). Super-elasticity properties enable Ni-Ti rotary files to be placed in curved canals exerting less lateral forces on the canal walls and maintaining the original canal shape (3,4). Ni-Ti rotary tools have unique design properties in terms of cross sectional shape, taper, tip and number and angle of flutes. These properties improve the shaping process without creating canal aberrations, particularly in narrow and severely curved canals (2). Preserving root canal anatomy represents a major issue difficult to overcome. Despite this, several studies showed that shaping outcomes with nickel-titanium rotary instruments are generally predictable (5,6). Coronal enlargement and manual or mechanical pre-flaring to create a glide path was demonstrated to be the first step for a safer use of Ni-Ti rotary instrumentation, because it prevents fractures of torsion instruments and shaping aberrations (7-9). Recently, Ni-Ti rotary PathFiles (PFs) were introduced to improve mechanical pre-flaring (7,10). These instruments are more capable of maintaining the original canal anatomy and cause less aberrations and modifications of canal curvature compared to manual pre-flaring performed with stainless-steel KF (7). Of note, clinician's expertise did not appear to have a significant impact on outcome (7). A number of techniques were utilized to evaluate endodontic instrumentation (3), such as plastic models (11), histological sections (12), scanning electron microscopic studies (13), serial sectioning with Bramante technique (14), radiographic comparisons (15) and silicon impressions of instrumented canals (16). X-ray micro-computed-tomography (CT) scanners are based on cone-beam geometry and are optimized to obtain non-destructive high-resolution (from 1 to tens of microns) 3D imaging of small objects. The main component of this scanner is the micro-focus X-ray source featuring a spot size of less than 50 microns (usually only a few microns). Differently from the medical CT, the specimen is mounted on a high precision rotation stage and revolves around its own axis, while the X-ray source and the detector are steady. The 3D reconstruction of the data is usually based on Feldkamp algorithm (17). Micro-CT has recently emerged as a powerful tool for evaluation of root canal morphology. This non-invasive technique allows a

detailed 3D evaluation of the effects of canal preparation on anatomy (18). It also allows the superimposition of 3D renderings of pre-operative and post-operative canal system with a high resolution. In this study we aimed to compare the ability of manual and mechanical glide path to maintain the original root canal anatomy by using the micro-CT technique.

MATERIALS AND METHODS

Eight extracted upper first permanent molars with fully-formed apex that had not undergone prior endodontic treatment were used. After debriding the root surface, specimens were immersed in a 5% solution of NaOCl (Niclor 5, OGNA, Muggiò, Italy) for 1 hour and then stored in saline solution.

Micro-CT analysis

Specimens were mounted on a stable support and then scanned at the TOMOLAB station (19) at ELETTRA Synchrotron Light Laboratory in Trieste (Italy). The system is a cone beam geometry with the following characteristics: (a) sealed tungsten micro-focus X-ray tube, with a focal spot size ranging from 5 to 40 microns, an energy ranging from 40 to 130 kV and a maximum current of 300 microA; (b) a water cooled CCD camera with a large field of view (49.9 mm×33.2 mm) and a small pixel size (12.5×12.5 microns2). A total number of 2400 projections on 360° at 100 kV and 80 μA, focal spot size of 8 microns, with a focus-object and focus-detector distance of 110 mm and 300 mm respectively, in a time frame of 2 hours and 32 minutes for each specimen were acquired.

Axial images were reconstructed by means of Cobra 7.2 software (Exxim, Pleasanton, CA, USA) and subsequently elaborated for artifacts removal using PORE3D (20), a software developed at the Elettra research center. High resolution raw 16 bit images were converted to 8 bit TIFF file format; the whole stack gives a volume of around 1000x1000x1000 isotropic voxels featuring 9.2 micron side length. Each image stack was first equalized by ImageJ 1.43u 64 bit (a freeware software by

the National Institute of Health, U.S.A.) and then processed by Amira 5.3.3 64 bit edition (Visage Imaging, Richmond, Australia) for volume registration and cutting plane selection. The registration algorithm was based on the mean square difference between the gray values of the two image sets. The alignment steps have been set to 0.9 microns with a tolerance of 0.0001 units on the voxel intensity.

Each root canal path was studied dynamically by examining both high resolution 3D rendering and orthogonal cross-sections. Root sections orthogonal to the canal axis were set at two different levels: at 1 mm from the canal apex (A); and at the point of maximum curvature (C). The cutting plane orientation was the same for both the pre and post- treatment samples. This axial sections have been imported in TIFF format and analyzed with ImageJ to measure area, perimeter and diameters (major and minor, orthogonal to one another), by using an automatic thresholding algorithm to avoid manual errors. Measurements were performed twice by the same operator (intra-observer control) and once by another operator (inter-observer control).

Specimen preparation

After access cavity preparation, working length (WL) was established under microscopic vision (OPMI Pro Ergo, Carl Zeiss, Oberkochen, Germany) at 10X magnification, when the tip of a #10 KF was visible at the root tip. Buccal root canals (MB1 and DB) of each specimen were randomly assigned to PF test group or stainless-steel KF control group.

In the PF test group, the mechanical glide path was performed by using Glyde™ (Dentsply Maillefer, Ballaigues, Switzerland) as lubricating agent, with Ni-Ti rotary instruments PF 1, 2 and 3 (Dentsply Maillefer, Baillagues, Switzerland), by using an endodontic engine (X-Smart, Dentsply Maillefer, Baillagues, Switzerland) with 16:1 contra angle, at the suggested setting (300 rpm on display, 5 Ncm), at WL.

In KF control group, the manual glide path was carried out by using Glyde™ (Dentsply Maillefer, Ballaigues, Switzerland) as lubricating agent, with stainless-steel KF #08-10-12-15-17-20 (Dentsply Maillefer, Baillagues, Switzerland), used with "feed it in and pull" motion at WL. During treatment, irrigation with 5% NaOCl (Niclor 5, OGNA, Muggiò, Italy) was performed with a 30 gauge needle syringe for a total of 10 ml. Root canals were dried with sterile paper points and specimens were then micro-scanned as previously described for post-treatment analysis and comparisons.

The angles of curvature of the canals were calculated and classified as *moderate* (M, ≤ 35°) or *severe* (S, ≥ 40°). To evaluate canal modifications induced by preparation, two different geometric parameters were considered for the statistical analysis:

- the ratio of diameter ratios (RDR): i.e., $RDR=(D/d)_{post}/(D/d)_{pre}$, where $(D/d)_{post}$ is the post-preparation ratio of the major diameter (D) to the minor diameter (d), and $(D/d)_{pre}$ is the pre-preparation ratio of D to d;

- the ratio of cross-sectional areas (RA): i.e., $RA=A_{post}/A_{pre}$, where A_{post} and A_{pre} are the post-preparation and the pre-preparation cross-sectional areas, respectively.

For each level of analysis (A and C), two balanced two-way factorial ANOVA's were performed to evaluate the significance of the instrument factor (PF and KF) and of the canal curvature factor (M and S) at the two levels, as well as the interactions of these factors both with RDR and RA. To define RDR and RA parameters, 36 and 20 independent repetitions for each treatment combination were respectively performed.

Significance level was set to 5% ($p<0.05$). All statistical analyses were performed by using the Minitab 15 software package (Minitab Inc., State College, PA, USA)**.**

RESULTS

Specimens in the KF group had a mean curvature of 35.4°±11.5° (min=20°, max=55°), while specimens in the PF group had a mean curvature of 38°±9.9° (min=25°, max=55°).

Four balanced two-way factorial ANOVA's were performed and statistical significance of factors and interactions were evaluated by determining a total of 12 p-values:

- Instrument factor
    - at point A, $p<0.001$ for RDR parameter and $p=0.001$ for RA parameter;
    - at point C, $p<0.001$ for both RDR and RA parameters;
- Curvature factor
    - at point A, $p<0.001$ for RDR parameter and $p=0.751$ for RA parameter;
    - at point C, $p=0.045$ for RDR parameter and $p=0.011$ for RA parameter;
- Instrument-curvature interaction
    - at point A, $p=0.553$ for RDR parameter and $p=0.037$ for RA parameter;
    - at point C, $p<0.001$ for RDR parameter and $p=0.025$ for RA parameter.

Therefore instrument factor was found to be extremely significant both for the RDR and RA parameters, regardless of the point of analysis. The interval plots for the RDR parameter (Figure 2A) and for the RA parameter (Figure 2B) graphically confirm statistical significance of instrument factor. When PF is used, both the RDR and the RA parameters are closer to value 1, which means that canal modifications are statistically significantly reduced. The curvature factor significantly influenced both RDR and RA parameters, except for RA assessed at the point of analysis A (Figure 2). Finally, the interaction between factors significantly influenced RDR and RA, again except for RDR assessed at the point of analysis A (Figure 3).

DISCUSSION

Previous studies demonstrated that micro-CT used to evaluate root canals prepared with Ni-Ti hand or rotary instruments versus stainless-steel endodontic instruments provided a non-destructive and easy to repeat method (3,21). Micro-CT has been successfully used to evaluate performance of ProTaper Ni-Ti instruments on shaping root canals despite varied anatomies (22). Data obtained with micro-CT enable to identify morphological changes associated with different biomechanical preparations including canal transportation, dentin removal and final canal preparation (18,23,24). A major advantage of micro-CT is the possibility to obtain highly accurate evaluation of root canal shape by superimposition and measurement of 3D renderings (6,18,25). In the present study, micro-CT analysis confirmed findings of a previous study showing that Ni-Ti rotary PFs are more capable of maintaining original canal anatomy and cause less canal aberrations during instrumentation (7). Moreover, the impact of the instrument factor was significant in almost all interactions to canal curvature and point of analysis factors considered. PF instruments caused significantly less alteration of the canal anatomy, as evidenced by the analyses performed on the geometric variables. Preliminary manual or mechanical pre-flaring showed to be fundamental before safe rotary instrumentation because it preserves rotary instruments from excessive torsion stresses (7-9,26). Torsion stresses might increase dramatically if the area of contact between dentine walls and cutting edges of the instruments increases (27,28) or if the canal section is smaller than the non-active tip of the Ni-Ti rotary instruments and taper lock subsequently used (27-29). Maintaining the original canal shape using a less invasive approach is associated with better endodontic outcomes (6). Previous studies found that canal transportation leads to inappropriate dentine removal with high risk of straightening of the original canal curvature and formation of ledges in dentine wall, as well as excessive apical enlargement with hourglass appearance and subsequent defects in sealing (24,30). Outer apical transportation and foramen widening may increase the risk of lack of apical stop and extrusion of infected debris and microorganisms causing post-operative discomfort, thus jeopardizing endodontic treatment outcome (6,31-33). Studies demonstrated that obturated root

canals with irregular shapes leak significantly more compared with those with little or no canal transportation (34). Therefore, preserving the original canal shape and the lack of canal aberrations are associated with higher antimicrobial and sealing efficiency and do not excessively weaken tooth structure (35).

Within the limits of this study, our results confirmed that, by providing a pre-flaring with less canal transportation, Ni-Ti rotary PFs enable an optimal glide path for the Ni-Ti rotary instruments used afterwards. These instruments actually have high root canal centering ability, cause less modifications of the canal curvature and fewer canal aberrations. Therefore, PFs showed to preserve the original canal shape considerably better than manual stainless-steel instruments.

Conflict of interest: G. Cantatore, A. Castellucci, E. Berutti declare financial involvement (patent licensing arrangements) with Dentsply Maillefer with direct financial interest in the materials discussed in this manuscript.

Figure legends

Fig 1 A) 3D reconstruction of a specimen; B) Root canal path with selection of the cutting plane; C) Cutting plane orthogonal to the canal axis in the pre-treatment specimen; D) Same cutting plane in the post-treatment specimen; E) Image matching of the two radiological sections, according to the previously selected cutting plane, shows the difference of the canal diameters between the pre (red) and post-treatment (grey) specimens.

Fig 2 Interval plot for the ratio of diameter ratio (RDR) and ratio of cross-sectional areas (RA) parameters; 95% confidence intervals for the mean. M= moderate curvature; S= severe curvature; K= k-file instrument; P= Pathfile instrument; A= canal apex; C= point of maximum canal curvature;

Fig 3 Interaction plots for each ANOVA. a) ratio of diameter ratio (RDR) parameter evaluated at canal apex (A); b) ratio of cross-sectional areas (RA) parameter evaluated at point A; c) RDR parameter evaluated at point of maximum canal curvature (C); d) RA parameter evaluated at point C. Large non parallelism between solid and dashed lines is evidence of statistical significance of Interaction. M= moderate curvature; S= severe curvature; K= k-file instrument; P= Pathfile instrument.

REFERENCES

1. Javaheri HH, Javaheri GH. A comparison of three Ni-Ti rotary instruments in apical transportation. J Endod 2007;33:284-6.
2. Schäfer E, Vlassis M. Comparative investigation of two rotary nickel-titanium instruments: ProTaper versus RaCe. Part 2. Cleaning effectiveness and shaping ability in severely curved root canals of extracted teeth. Int Endod J 2004;37:239-48.
3. Gambill JM, Alder M, del Rio CE. Comparison of nickel-titanium and stainless steel hand-file instrumentation using computed tomography. J Endod 1996;22:369-75.
4. Coleman CL, Svec TA. Analysis of Ni-Ti versus stainless steel instrumentation in resin simulated canals. J Endod 1997;23:232-5.
5. Glossen CR, Haller RH, Dove SB, del Rio CE. A comparison of root canal preparations using Ni-Ti hand, Ni-Ti engine-driven, and K-Flex endodontic instruments. J Endod 1995;21:146-51.
6. Peters OA. Current challenges and concepts in the preparation of root canal systems: a review. J Endod 2004;30:559-67.
7. Berutti E, Cantatore G, Castellucci A, Chiandussi G, Pera F, Migliaretti G, Pasqualini D. Use of nickel-titanium rotary PathFile to create the glide path: comparison with manual preflaring in simulated root canals. J Endod 2009;35:408-12.
8. Patiño PV, Biedma BM, Liébana CR, Cantatore G, Bahillo JG. The influence of a manual glide path on the separation rate of NiTi rotary instruments. J Endod 2005;31:114-6.
9. Berutti E, Negro AR, Lendini M, Pasqualini D. Influence of manual preflaring and torque on the failure rate of ProTaper rotary instruments. J Endod 2004;30:228-30.
10. Gergi R, Rjeily JA, Sader J, Naaman A. Comparison of canal transportation and centering ability of twisted files, Pathfile-ProTaper system, and stainless steel hand K-files by using computed tomography. J Endod 2010;36:904-7.

11. Weine FS, Kelly RF, Lio PJ. The effect of preparation procedures on original canal shape and on apical foramen shape. J Endod 1975;1:255-62.
12. Walton RE. Histologic evaluation of different methods of enlarging the pulp canal space. J Endod 1976;2:304-11.
13. Mizrahi SJ, Tucker JW, Seltzer S. A scanning electron microscopic study of the efficacy of various endodontic instruments. J Endod 1975;1:324-33.
14. Bramante CM, Berbert A, Borges RP. A methodology for evaluation of root canal instrumentation. J Endod 1987;13:243-5.
15. Southard DW, Oswald RJ, Natkin E. Instrumentation of curved molar root canals with the Roane technique. J Endod 1987;13:479-89.
16. Abou-Rass M, Jastrab RJ. The use of rotary instruments as auxiliary aids to root canal preparation of molars. J Endod 1982;8:78-82.
17. Feldkamp LA, Davis LC, Kress JW. Practical cone-beam algorithm. J Opt Soc Am, 1984, A1:612–19.
18. Peters OA, Laib A, Göhring TN, Barbakow F. Changes in root canal geometry after preparation assessed by high-resolution computed tomography. J Endod 2001;27:1-6.
19. TOMOLAB—X-ray CT laboratory, 2010, www.elettra.trieste.it/Labs/TOMOLAB.
20. Brun F, Mancini L, Kasae P, Favretto S, Dreossi D, Tromba G. Pore3D: A software library for quantitative analysis of porous media. Nuclear Instruments and Methods in Physics Research, Section A: Accelerators, Spectrometers, Detectors, and Associated Equipment, 2010, v. 615 (3): 326–32.
21. Nair MK, Nair UP. Digital and advanced imaging in endodontics: a review. J Endod 2007;33:1-6.
22. Peters OA, Peters CI, Schönenberger K, Barbakow F. ProTaper rotary root canal preparation: effects of canal anatomy on final shape analysed by micro CT. Int Endod J 2003;36:86-92.

23. Paqué F, Ganahl D, Peters OA. Effects of root canal preparation on apical geometry assessed by micro-computed tomography. J Endod 2009;35:1056-9.
24. Loizides AL, Kakavetsos VD, Tzanetakis GN, Kontakiotis EG, Eliades G. A comparative study of the effects of two nickel-titanium preparation techniques on root canal geometry assessed by microcomputed tomography. J Endod 2007;33:1455-9.
25. Bjørndal L, Carlsen O, Thuesen G, Darvann T, Kreiborg S. External and internal macromorphology in 3D-reconstructed maxillary molars using computerized X-ray microtomography. Int Endod J 1999;32:3-9.
26. Roland DD, Andelin WE, Browning DF, Hsu GH, Torabinejad M. The effect of preflaring on the rates of separation for 0.04 taper nickel titanium rotary instruments. J Endod 2002;28:543-5.
27. Blum JY, Cohen A, Machtou P, Micallef JP. Analysis of forces developed during mechanical preparation of extracted teeth using Profile NiTi rotary instruments. Int Endod J 1999;32:24-31.
28. Peters OA, Peters CI, Schönenberger K, Barbakow F. ProTaper rotary root canal preparation: assessment of torque and force in relation to canal anatomy. Int Endod J 2003;36:93-9.
29. Yared GM, Bou Dagher FE, Machtou P. Influence of rotational speed, torque and operator's proficiency on ProFile failures. Int Endod J 2001;34:47-53.
30. Jafarzadeh H, Abbott PV. Ledge formation: review of a great challenge in endodontics. J Endod 2007;33:1155-62.
31. Siqueira JF Jr, Rôças IN, Favieri A, Machado AG, Gahyva SM, Oliveira JC, Abad EC. Incidence of postoperative pain after intracanal procedures based on an antimicrobial strategy. J Endod 2002;28:457-60.
32. Seltzer S, Naidorf IJ. Flare-ups in endodontics: I. Etiological factors. 1985. J Endod

2004;30:476-81;discussion 475.

33. Vaudt J, Bitter K, Neumann K, Kielbassa AM. Ex vivo study on root canal instrumentation of two rotary nickel-titanium systems in comparison to stainless steel hand instruments. Int Endod J 2009;42:22-33.
34. Wu MK, Fan B, Wesselink PR. Leakage along apical root fillings in curved root canals. Part I: effects of apical transportation on seal of root fillings. J Endod 2000;26:210-6.
35. Moore J, Fitz-Walter P, Parashos P. A micro-computed tomographic evaluation of apical root canal preparation using three instrumentation techniques. Int Endod J 2009;42:1057-64.

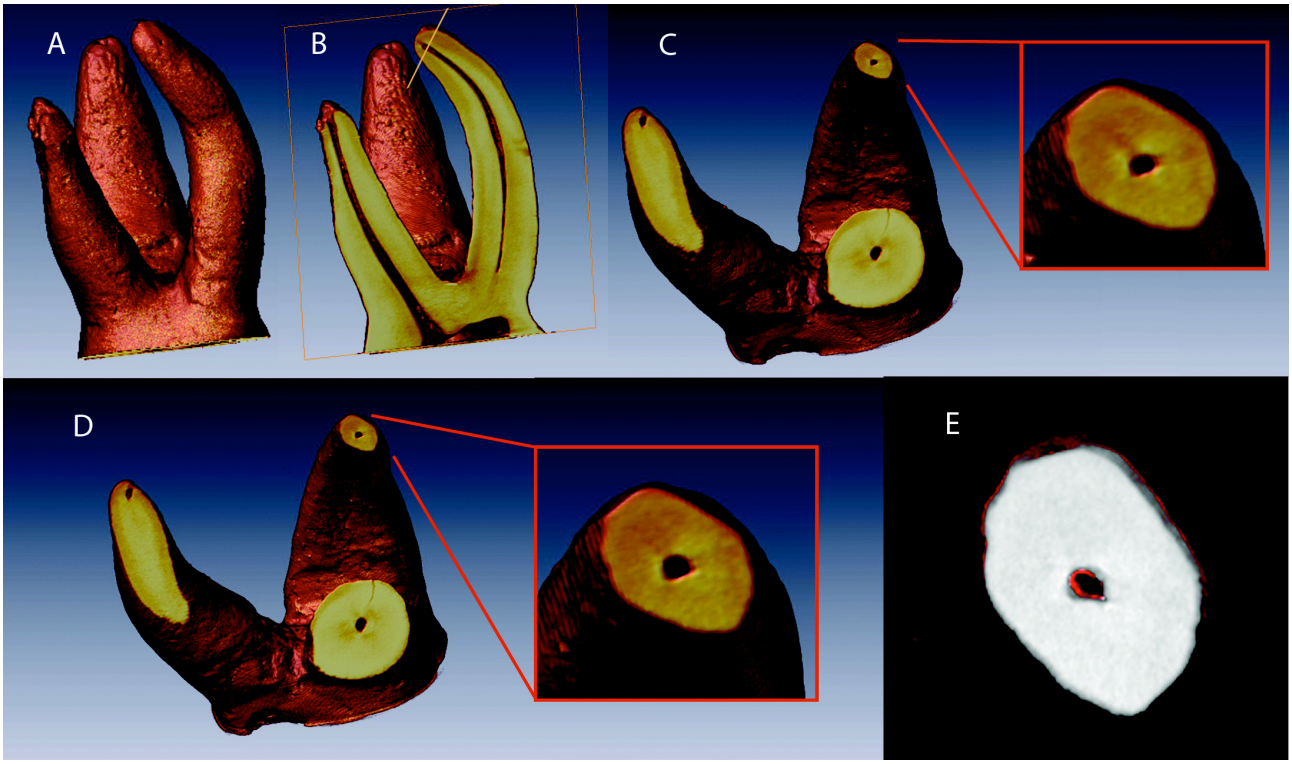

Fig 1 A) 3D reconstruction of a specimen; B) Root canal path with selection of the cutting plane; C) Cutting plane orthogonal to the canal axis in the pre-treatment specimen; D) Same cutting plane in the post-treatment specimen; E) Image matching of the two radiological sections, according to the previously selected cutting plane, shows the difference of the canal diameters between the pre (red) and post-treatment (grey) specimens.

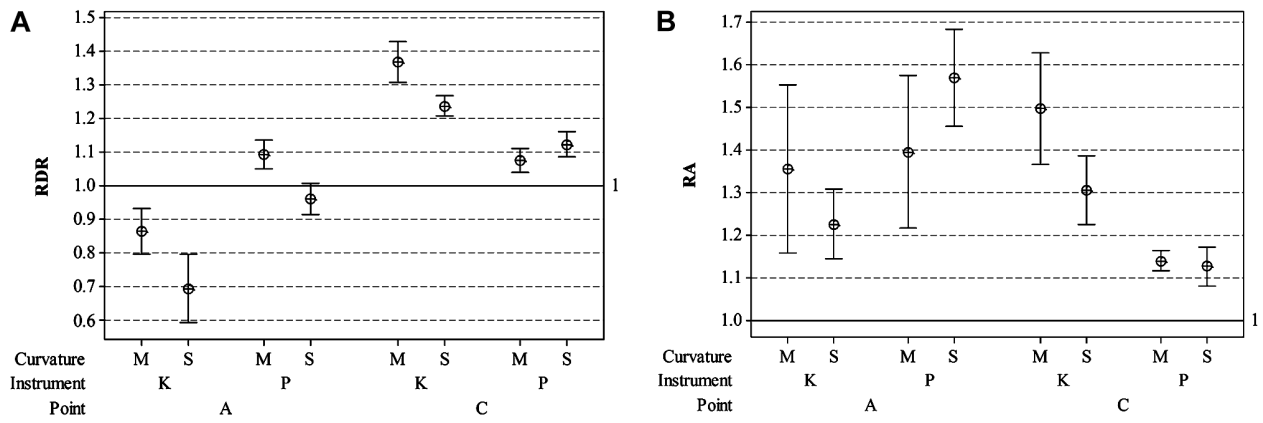

Fig 2 Interval plot for the ratio of diameter ratio (RDR) and ratio of cross-sectional areas (RA) parameters; 95% confidence intervals for the mean. M= moderate curvature; S= severe curvature; K= k-file instrument; P= Pathfile instrument; A= canal apex; C= point of maximum canal curvature;

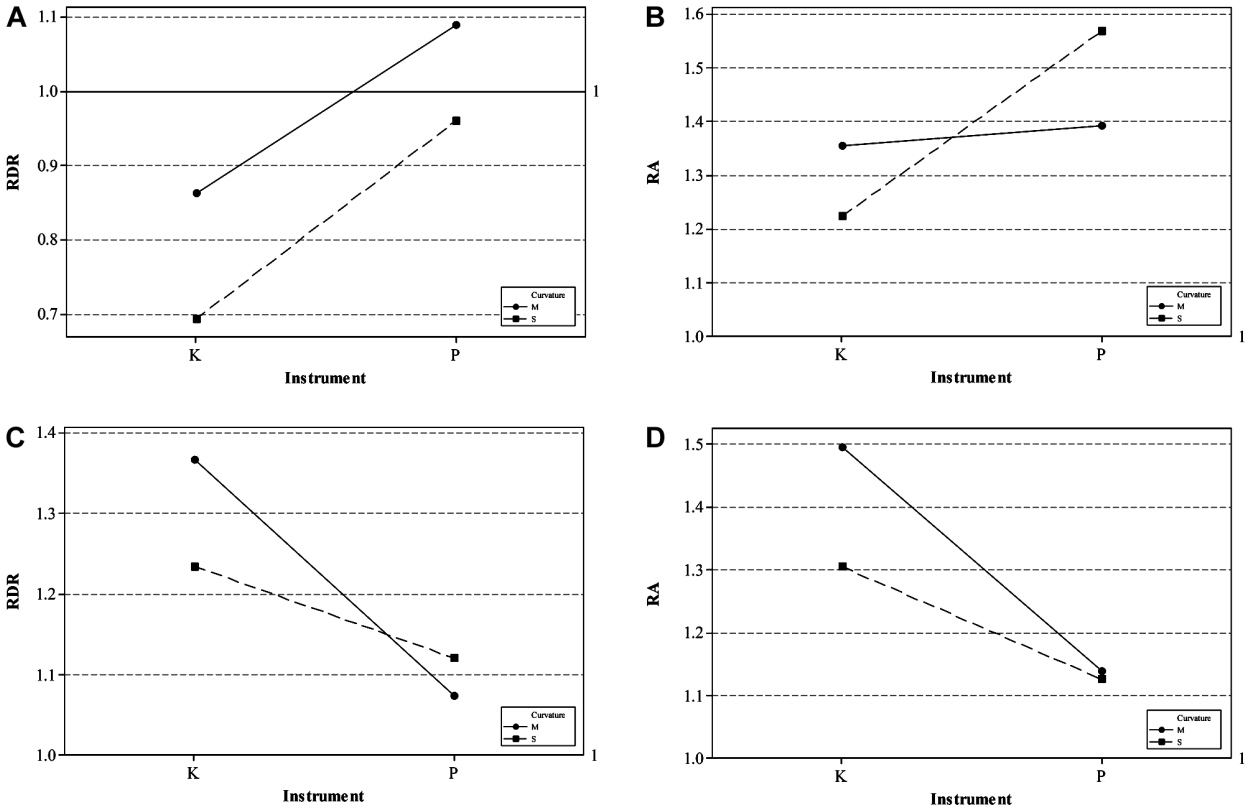

Fig 3 Interaction plots for each ANOVA. a) ratio of diameter ratio (RDR) parameter evaluated at canal apex (A); b) ratio of cross-sectional areas (RA) parameter evaluated at point A; c) RDR parameter evaluated at point of maximum canal curvature (C); d) RA parameter evaluated at point C. Large non parallelism between solid and dashed lines is evidence of statistical significance of Interaction. M= moderate curvature; S= severe curvature; K= k-file instrument; P= Pathfile instrument.